

1. Title Page.

Evaluation of ADMET PredictorTM in early discovery DMPK project
work

Anna-Karin Sohlenius-Sternbeck and Ylva Terelius

Previous address: Medivir AB, P.O Box 1086, SE-141 22 Huddinge, Sweden (A.S., Y.T.)

Present address: Research Institutes of Sweden, RISE, SE-151 36 Södertälje, Sweden (A.S.)

and ADMEYT AB, SE-179 62 Stenhamra, Sweden (Y.T.)

2. Running Title Page.

- a) Running Title: ADMET Predictor™ in early discovery DMPK project work
- b) Corresponding author: Anna-Karin Sohlenius-Sternebeck, Research Institutes of Sweden, RISE, SE-151 36 Södertälje, Sweden. Email: anna-karin.sternebeck@ri.se;
Telephone number: +46 70 309 63 49

- c) Number of text pages: 23

Number of tables: 9 (including Supplemental Tables 1 to 4)

Number of figures: 5

Number of references: 20

Number of words in the Abstract: 249

Number of words in the Introduction: 778

Number of words in the Discussion: 1365

- d) List of nonstandard abbreviation:

ABBA, apical to basolateral and basolateral to apical; ADME, absorption, distribution, metabolism, excretion; ANN, artificial neural network; AP, ADMET Predictor™; CL_{int} , in vitro intrinsic clearance; CYP, cytochrome P450; DMPK, drug metabolism and pharmacokinetics; GF, GF120918 (Elacridar); HLM, human liver microsomes; HPLC, high performance liquid chromatography; MAE, mean absolute error; P_{eff} , effective jejunal permeability; P_{app} , apparent permeability; P-gp, P-glycoprotein; PK, pharmacokinetic; PKPD, pharmacokinetic-pharmacodynamic; QSAR quantitative structure-activity relationship; QSPR, quantitative structure–property relationship; RMSE, root mean square error.

3. Abstract.

A dataset consisting of measured values for LogD, solubility, metabolic stability in human liver microsomes (HLM) and Caco-2 permeability was used to evaluate the prediction models for lipophilicity (S+LogD), water solubility (S+Sw_pH), metabolic stability in HLM (CYP_HLM_Clint), intestinal permeability (S+Peff) and P-gp substrate identification (P-gp substrate) in the software ADMET Predictor™ (AP) from Simulations Plus. The dataset consisted of a total of 4794 compounds, with at least data from metabolic stability determinations in HLM, from multiple discovery projects at Medivir. Our evaluation shows that the global AP models can be used for categorization of high and low values based on predicted results for metabolic stability in HLM and intestinal permeability, and to give good predictions of LogD ($R^2=0.79$), guiding the synthesis of new compounds and for prioritizing in vitro ADME experiments. The model seems to overpredict solubility for the Medivir compounds, however. We also used the in-house datasets to build local models for LogD, solubility, metabolic stability and permeability by using artificial neural network (ANN) models in the optional Modeler™ module of AP. Predictions of the test sets were performed with both the global and the local models and the R^2 value for linear regression for predicted versus measured HLM CL_{int} based on logarithmic data was 0.72 for the in-house model and 0.53 for the AP model. The improved predictions with the local models are likely explained both by the specific chemical space of the Medivir dataset and lab specific assay conditions for parameters which require biological assay systems.

4. Significance Statement.

AP is useful early in projects for predicting and categorizing LogD, metabolic stability and permeability, to guide the synthesis of new compounds and for prioritizing in vitro ADME experiments. The building of local in-house prediction models with the optional AP Modeler Module can give improved prediction success since these models are built on data from the same experimental setup and can also be based on compounds with similar structures.

5. Visual abstract.

See separate image file.

6. Introduction.

In vivo drug disposition is dependent on the interactions between the drug and the body. During the drug discovery phase, chemical synthesis is guided towards potent compounds with physicochemical and ADME (absorption, distribution, metabolism and excretion) properties that allow the drug to reach effective concentrations at the target (Ballard et al., 2012; Sohlenius-Sternbeck et al., 2016). Also, compounds should show low toxicity (Kramer et al., 2007). Early characterization and understanding of the properties of new chemical entities facilitate the further optimization of a chemical series toward a new drug candidate.

Reliable in silico prediction tools for ADME properties can help decision making in the early phase of drug discovery, even before experimental data is available (van de Waterbeemd, 2003; Moda, 2008; Wang et al., 2015; Alqahtani, 2017; Kazmi et al., 2018; Stålring et al., 2018). With such tools, the chemical design and synthesis can be prioritised and focus on compounds with the best potential to show desired properties later in vivo. The building of quantitative structure-activity /quantitative structure–property relationships (QSAR/QSPR) models is highly dependent on the quality of the training set data (Gleeson and Montanari, 2012). Moreover, metabolism, distribution and excretion involve multi-mechanistic processes which make the building of in silico models challenging.

The use of a commercial software for predictions of chemical and ADMET properties is convenient, since such tools can be used with virtual compounds and do not require any user data while measured data is needed for local model building. However, in the commercial models, the chemical space of the local compounds may not be covered. It is also likely that commercial models are built on datasets from multiple sources with dissimilarities in the experimental setup. For many assays, the experimental variability between different laboratories is substantial (Hayeshi, 2008; Liu, 2015), which often makes it desirable to build

in-house local models. A local model would also better cover the chemical space of in-house compounds, especially within a project/project series with similar structures, and the user can have control over the training set. However, when building in-house models, a big enough training set with good quality data covering the chemical space, is needed. For these reasons, large pharmaceutical companies have their own dedicated modelers responsible for building in-house project specific QSAR/QSPR models.

Several commercial softwares or online prediction tools are available for ADME, PK, PKPD, DDI (drug-drug interactions) and toxicity predictions. We have previously successfully used GastroPlus™ from Simulations Plus as part of a strategy to identify risks for DDI in drug discovery (Sohlenius-Sternbeck et al., 2018). ADMET Predictor™ (AP) from SimulationsPlus Inc is a commercially available software for prediction of physical chemistry, ADME and toxicity parameters from compound structures. In this work, we used a dataset with experimental in-house data to evaluate whether the global models in the commercially available AP software can be used as tools in early drug discovery (before in-house data is available). The parameters predicted were water solubility, lipophilicity, metabolic stability in human liver microsomes (HLM), permeability and whether a compound will be a substrate for P-gp. Included in the study were 4794 compounds in the Medivir database with metabolic stability data in HLM. The dataset consists of compounds from multiple discovery projects at Medivir and it comprises mainly protease inhibitors and nucleoside analogues which may not be well represented in the training set for the global models. We evaluated the AP models for LogD (S+LogD), water solubility (S+S_pH), metabolic stability in HLM (CYP_HLM_Clint), permeability (S+Peff) and P-gp substrate (Yes/No) by comparing predicted values with experimental results.

The ADMET Modeler™ tool is an optional module in AP and can be used to build local and/or project specific models based on QSAR/QSPR and by using chemical descriptors obtained with the AP software. The module is licensed separately and can be used without extensive knowledge in modelling. With the ADMET Modeler Module™, local ANN models for Log D, solubility, metabolic stability and permeability were built using the Medivir dataset, and the models were tested on in-house compounds as well as on commercially available reference compounds. The outcome of the local in-house models was compared with the outcome of the global AP models. A good training set is required for a predictive outcome and the larger and the more similar the structures in the training set the better the predictive outcome, but we have previously built local models for projects in Lead Optimization phase based on training sets of about 20 similar compounds from a single compound series. These were useful and predictive for the next round of synthesis but had to be rebuilt often as the results were used to improve the structures, moving away from the training set structures (unpublished results).

7. Materials and Methods.

Chemicals

All chemicals were of analytical grade and obtained from commercial suppliers.

Characteristics of the Medivir dataset

The vast majority of the compounds in the Medivir dataset had a purity $\geq 95\%$ according to HPLC analysis (no compound had a purity $\leq 80\%$). Compounds observed to be chemically unstable or poorly soluble during the experiments were removed (i.e., 78 compounds). The distribution of molecular weight (of the remaining 4794 compounds) and measured LogD (1198 compounds) for the Medivir compounds are shown in Figure 1A and B, respectively. There were 2236 zwitterions, 1888 bases, 623 acids, 44 neutrals and 3 compounds with mixed pKa values in the dataset. Most of the acids were weak with pKa values above 7 (only 52 acids had a pKa below 5). Also, most of the bases were weak bases with pKa below 7 (only 385 bases had a pKa above 8).

Predictions of ADME properties

Predictions of ADME properties were made using the ADMET PredictorTM software, here called AP (version 9.5, SimulationsPlus Inc, Lancaster, CA; <http://www.simulations-plus.com>), and the chemical structures were defined by SMILES. The software models for LogD (S+LogD), water solubility (S+Sw_pH, i.e., solubility at a certain chosen pH, here pH 7.4), metabolic stability (CYP_HLM_Clint), effective jejunal permeability (S+Peff) as well as P-gp substrate identification were evaluated using the Medivir dataset.

Moreover, in-house local models were built on training sets from the Medivir dataset, using artificial neural network ensembles (ANNE) in the optional ADMET ModelerTM module (Modeler). The Modeler uses an early stopping technique, in which the interplay between the model complexity and quality of output are taken into account to avoid the

generation of an overtrained model. The in-house models for solubility, HLM CL_{int} and Caco-2 permeability were based on logarithmic data. A training set that represented approximately 75-80% of the measured values was used for each parameter, and the remaining 20-25% was used as a test set to evaluate the model. The test sets were selected in the ADMET Modeler™ module based on Kohonen mapping (Yan and Gasteiger, 2003). The test sets were also evaluated in the corresponding ADMET Predictor™ software global models. Each model was rebuilt at least four times and the deviation for each statistical parameter (see the statistical section) was around 10% or less between the models. Tables and figures show data from one representative model for each assay.

Determination of LogD

Determination of LogD was performed for Medivir by GVK Biosciences Limited (Hyderabad, India). LogD was determined by measuring the partition coefficient between water and octanol at pH 7.4. Fifteen μL of test compound stock solution (10 mM in DMSO) was added to 500 μL octanol in 3 replicates and vortexed for 10 min on a plate shaker at 1200 rpm. 500 μL 10 mM phosphate buffer, pH 7.4, was added and the mixture vortexed for another hour at 1200 rpm. The samples were allowed to settle for 20 min and then centrifuged at 4000 rpm for 30 min at room temperature for complete phase separation and analysed by HPLC-UV absorbance.

Determination of kinetic solubility

Kinetic solubility measurements were also performed at GVK Biosciences Limited (Hyderabad, India). A stock solution of 10 mM compound in DMSO was added to 10 mM phosphate buffered saline, pH 7.4, to give a final compound concentration of 100 μM in 10 mM phosphate with 1% DMSO. After a period of vigorous vortexing, the precipitate was removed by vacuum filtration. No correction for non-specific binding was performed. The compound concentration in the resulting filtrate was determined by HPLC-UV absorbance.

The kinetic solubility assay could not generate solubilities above 100 μM since that was the final concentration added in the assay. Thus, higher solubilities were reported as $> 100 \mu\text{M}$.

Determination of permeability

Permeability in Caco-2 cells (Artursson et al., 2001) was assayed at Medivir or at GVK Biosciences Limited (Hyderabad, India) using the same assay setup (also evaluated with reference compounds) as described below. Caco-2 cells, at passage number 36, were used in the transport experiments. The cells were purchased from American Type Culture Collection (Middlesex, UK). Caco-2 cells were seeded in 96 well plates (12000 cells/well) and cultured for 21 days on cell culture transwell inserts (Transwell). The integrity of the cell monolayer was determined using Lucifer yellow measured in an Envision multilabel Reader at Ex/Em 428/535 nm. Trans epithelial electrical resistance (TEER) was also measured to determine the integrity of the cell barrier. The TEER value was above $230 \text{ ohms} \times \text{cm}^2$ in all experiments.

The permeability of the test compound (at 10 μM) over a Caco-2 cell monolayer from the apical to the basolateral compartment (A to B) was investigated in duplicates over a period of 120 minutes. Hank's Balanced salt solution (HBSS), pH 6.5, containing 25 mM morpholino ethane sulfonic acid (MES) was used as apical buffer, and HBSS, pH 7.4, containing 25 mM hydroxy ethyl piperazine ethane sulfonic acid (HEPES) and 1% bovine serum albumin (BSA) as basolateral buffer. The test compound (10 μM) in apical buffer was added to the apical well. Incubation was performed at 37°C, and the plates were kept shaking at approximately 150 rpm. At time point 30 min, an aliquot of basolateral sample was collected and replenished with same volume of basolateral buffer. At 120 min, samples were collected from basolateral and apical chamber. The donor samples were diluted with basolateral buffer (1:1, v/v) and the receiver samples were diluted with apical buffer (1:1, v/v). Possible efflux of test compound was investigated by blocking the MDR1 and BCRP efflux pumps in the A to B assay using 5 μM GF120918 (Elacridar).

In ABBA experiments, the bidirectional permeability of test compound (at 10 μ M) through a Caco-2 cell monolayer from the apical to the basolateral compartment and from the basolateral to the apical compartment was investigated in duplicate samples over a period of 120 minutes. HBSS, pH 7.4, containing 25 mM HEPES was used as buffer in the ABBA experiments. The test compound (10 μ M) in ABBA buffer was added to apical wells (A-B experiment) and to basolateral wells (B-A experiment). Aliquots were collected and treated in the same manner as described above.

All samples were precipitated with four volumes acetonitrile, containing losartan as internal standard, and vortexed for 5 min at 1000 rpm, followed by centrifugation at 4000 rpm for 10 min. Aliquots of the supernatants were analyzed by LC-MS/MS (see below).

The apparent permeability was calculated as follows:

$$P_{app} = \frac{dQ/dt}{C_0 \times A} \quad \text{Equation 1}$$

Where C_0 is the donor concentration at time 0 and A is the surface area and dQ/dt is the total amount of test compound transported across the cells per unit time.

Estimated +GF/-GF ratios of >1.5 and efflux ratios >2 were considered as an indication of efflux, based on validation using a set of reference P-gp substrates (Giacomini et al., 2010).

Determination of CL_{int}

Determination of the intrinsic clearance, CL_{int} , in HLM was performed at Medivir or at GVK Biosciences Limited (Hyderabad, India) using identical assay setup (also evaluated with reference compounds) as described below. Pools of HLM from 50 donors (mixed genders)

were purchased from XenoTech, LLC (Kansas City, US) and stored at -80°C. The microsomes were diluted in 100 mM phosphate buffer, pH 7.4. The final concentrations were 1 µM test compound and 0.5 mg microsomal protein per mL. Duplicate samples were pre-incubated for 10 min at 37°C before starting the reactions by the addition of NADPH to a final concentration of 1 mM (the total incubation volume was 250 µL). The incubations were stopped by the removal of aliquots (25 µL) at 0, 5, 15, 30 and 45 minutes to 96-well plates on ice containing 200 µL of stop solution to precipitate proteins. The stop solution, ice-cold acetonitrile, contained losartan (100 nmol/L) as an analytical internal standard. Samples were left on ice for at least 30 minutes to precipitate the microsomal proteins before removing the precipitate by centrifugation for 20 min at 2250 g. Aliquots of the supernatants were analysed by LC-MS/MS (see below).

The CL_{int} values were obtained from the disappearance curves where the substrate concentration was plotted against the time. The concentration of each test compound in the incubation was fitted to a first-order elimination equation

$$C = C_0 \cdot e^{-k \cdot \Delta t}, \quad \text{Equation 2}$$

where C is the measured concentration at time t , C_0 is the concentration at time 0 and k is the elimination constant. Curve fit was performed after natural logarithm transformation of the concentration data.

Intrinsic clearance was calculated as follows:

$$CL_{int} = k \cdot V \quad \text{Equation 3}$$

where V is the volume of the microsomal incubation.

The AP model for metabolic stability in microsomes (CYP_HLM_Clint) is based on the free concentration in the incubation. Since the measured CL_{int} values are based on total

concentrations and the fraction unbound in microsomes was not known, the predicted values obtained using the AP model were converted to total as follows:

$$Total CL_{int} = Unbound CL_{int} \times (S + fu_{mic}) \quad \text{Equation 4}$$

where $S+fu_{mic}$ is the predicted fraction unbound in the microsomal incubation (AP model).

The $S+fu_{mic}$ model is largely based on a publication by Austin et al. (2002).

Bioanalysis

The test compounds in the CL_{int} and permeability assays were quantified by LC/MS-MS (Sciex AB, Stockholm, Sweden or Shimadzu, India), in principle as described by Sohlenius-Sternbeck et al. (2010). The compounds were detected in positive or negative electrospray multiple reaction monitoring mode. Optimizations (parent ion and fragment determination, declustering potentials and collision energy) had been performed in advance.

Quality controls

Since the different assays were run in early screening, project compounds were run in 1 or 2 separate experiments. Reference compounds were always included in the different experiments as quality controls and to confirm reproducibility over time and between the Medivir and GVK Bio laboratories. Ketoconazole, metoprolol and propranolol were used as quality controls in every LogD experiment, since the LogD range of these compounds covers the LogD for most Medivir compounds. Albendazole and diethylstilbestrol were used as quality controls for solubility since these compounds cover the low concentration range ($\leq 10 \mu\text{M}$) applied in most in vitro ADME assays, and flurbiprofen was chosen as a quality control for high solubility. Atenolol, digoxin and propranolol were used as permeability quality controls, since these compounds cover the low to high permeability range. Digoxin and quinidine were used as quality controls for efflux in every Caco-2 + GF experiment and in every ABBA experiment. As a quality control in all HLM experiments each experiment

included incubations containing a cocktail of probe substrates for human drug-metabolizing enzymes, i.e., phenacetin (for CYP1A2), diclofenac (CYP2C9), bufuralol (CYP2D6) and midazolam (CYP3A4). Criteria for rejecting an experiment was based on whether data was outside two standard deviations of the Manhattan mean. Only project data from accepted experiments were used. For quality control data obtained in the different assays see Supplemental Tables 1A-E.

Bin categorization

Bin categorization was performed to evaluate the solubility, metabolic stability and permeability predictions. For solubility, bin A contained compounds with poor solubilities ($< 10 \mu\text{M}$) that might precipitate in the in vitro assays and bin D “good” solubilities ($>90 \mu\text{M}$, close to the added final concentration in the assay), which should suffice for most discovery studies except safety studies. Two other bins were created for practical reasons since some in vitro assays at Medivir were performed at up to $50 \mu\text{M}$.

In early discovery, we did not apply strict cut-offs for CL_{int} values, since the compounds are often improved in the optimization phase. A HLM CL_{int} value less than $15 \mu\text{L}/\text{min}/\text{mg}$, was considered stable enough (bin A) to be of interest. A CL_{int} value higher than $50 \mu\text{L}/\text{min}/\text{mg}$ can be considered to predict a low bioavailability over the liver, but since there is a fairly large uncertainty in the predictions, we raised the cut-off for bin D to $> 80 \mu\text{L}/\text{min}/\text{mg}$. Predicted values between 15 and $80 \mu\text{L}/\text{min}/\text{mg}$ were arbitrarily divided into 2 bins to differentiate between closer to “stable” (15 - $30 \mu\text{L}/\text{min}/\text{mg}$, bin B) and closer to “unstable” (30 - $80 \mu\text{L}/\text{min}/\text{mg}$, bin C).

The measured P_{app} values were also divided into 4 categories, A-D (<2 , 2 - 5 , 5 - 10 and $>10 \times 10^{-6} \text{ cm}/\text{s}$) and the corresponding categories A-D used for P_{eff} predictions were <1 ,

1-2, 2-3 and >3 (10^{-4} cm/s). The bin borders were set based on historic inhouse data for reference compounds.

Statistics

The root-mean-square error, RMSE, was calculated as a measure of the error of a model according to the equation below.

$$RMSE = \sqrt{\frac{\sum_{i=1}^N (Predicted - Observed)^2}{N}} \quad \text{Equation 5}$$

Where N is the number of compounds in the dataset.

The mean absolute error, MAE, was calculated as a measure of the mean absolute difference between predicted and observed data according to the equation below.

$$MAE = \frac{\sum_{i=1}^N \text{abs}(Predicted - Observed)}{N} \quad \text{Equation 6}$$

Criteria for accepting an experiment

The mean \pm SD values for each quality control, obtained from at least 12 independent measurements, were used to define whether or not an experiment could be accepted. An experiment was rejected if data was outside two standard deviations of the Manhattan mean.

Confusion tables for calculation of precision, sensitivity, specificity and accuracy

For the 2 \times 2 confusion tables based on P-gp “Yes/No” and Caco-2 P_{app} or ABBA, the precision, sensitivity, specificity and accuracy were calculated, where TY is predicted True “Yes”, TN is predicted True “No”, FY is predicted False “Yes” and FN is predicted False “No”.

Precision (or predictive value) is the proportion of predicted “Positives” that are true “Positives”:

$$Precision = \frac{Predicted\ TY}{(Predicted\ TY + Predicted\ FY)} \quad \text{Equation 7}$$

Sensitivity (or recall) is the proportion of actual “Positives” that were correctly predicted:

$$Sensitivity = \frac{Predicted\ TY}{(Predicted\ TY + Predicted\ FN)} \quad \text{Equation 8}$$

Specificity is the proportion of actual “Negatives” that were correctly predicted:

$$Specificity = \frac{Predicted\ TN}{(Predicted\ TN + Predicted\ FY)} \quad \text{Equation 9}$$

Accuracy is the proportion of data that was correctly predicted:

$$Accuracy = \frac{(Predicted\ TY + Predicted\ TN)}{(Predicted\ TY + Predicted\ TN + Predicted\ FY + Predicted\ FN)} \quad \text{Equation 10}$$

For the 4×4 confusion tables for the 3 models built with 4 categories (solubility, metabolic stability and permeability), precision (predictive value) and sensitivity (recall) were calculated for each bin. The F1-score for each bin is the harmonic mean of precision and recall, i.e.,

$$F1 - score = \frac{2 \times precision \times recall}{(precision + recall)} \quad \text{Equation 11}$$

The bin sizes, for the total data set as well as for the test set for each model, are shown in Table 1. Since we had unbalanced categories, we also used the Weighted F1 for overall “accuracy”, which takes the weighted mean of the individual F1-scores, considering the number of values in each measured category, i.e. the sum of the F1-scores for each measured category times the number of compounds in that category divided by the total number of compounds in the dataset.

$$\text{Weighted F1} = ((F1_A \times \text{measured cpds}_A) + (F1_B \times \text{measured cpds}_B) + (F1_C \times \text{measured cpds}_C) + (F1_D \times \text{measured cpds}_D)) / (\text{measured cpds}_A + \text{measured cpds}_B + \text{measured cpds}_C + \text{measured cpds}_D) \quad \text{Equation 12}$$

8. Results.

LogD predictions

The total number of compounds with measured LogD was 1198. Figure 2A shows the S+LogD, predicted by the global model provided in AP, versus the observed LogD for all compounds. The R^2 value was 0.79 (See also Table 2). A local, in-house model, based on a training set (911 compounds) from the Medivir data was built using the AP Modeler module, and Figure 2B shows the predicted LogD versus the observed LogD when this local model was used for the 287 compounds in the test set. The same test set was also predicted with the global AP model, S+LogD (Figure 2C). The R^2 values, when performing linear regression for the predicted values versus the measured values for the test set, using the S+LogD and the in-house LogD model were 0.79 and 0.89, respectively (Table 2).

Solubility predictions

The total number of compounds with measured solubility was 2778. The measured solubilities were divided into 4 categories, A-D (<10, 10-50, 50-90 and >90 μM) and the same categories were used for binning the predictions and a 4 \times 4 confusion table constructed. 55% of all measured values were in the highest category, i.e., >90 μM , and 21% in the lowest category, i.e., <10 μM (Table 1). When using the global AP model for all 2778 compounds, <3% (i.e., 69 compounds) had a predicted solubility of <10 μM (Table 1). Almost 82% of all compounds were predicted to have a solubility >90 μM . However, 56% of all compounds

were correctly predicted, when taking all categories into consideration, and many were close to the border between the categories (Table 3).

A training set consisting of 2087 of the compounds was used to build an in-house local solubility model using the AP Modeler module. The remaining 691 compounds were the test set. 71 of the 101 compounds (70%) that had a measured solubility $<10\ \mu\text{M}$ were also predicted to be poorly soluble ($<10\ \mu\text{M}$, See Figure 3B and Table 3). Only 12% of the highly soluble ($>90\ \mu\text{M}$) compounds were predicted to have solubility $>90\ \mu\text{M}$ but 73% were predicted to have a fairly high solubility (50-90 μM , See Figure 3B).

Table 2 summarizes the statistics for the linear regression for the plot of predicted versus measured solubility based on logarithmic data for these compounds. The R^2 value was 0.59 for the in-house model and lower for the AP model (i.e., 0.20 for the test set and 0.26 when using all compounds). The Precision (Predictive value), Sensitivity (Recall) and F1-score (per bin) for the categories and the overall accuracy (and Weighted F1) for all models are presented in Table 3. With the global model, the precision (or predictivity) was similar for bin A (low solubility, $<10\ \mu\text{M}$) and bin D (high solubilities, $>90\ \mu\text{M}$) with values between 0.54 and 0.68 when using all compounds or just the test set, indicating that the test set was representative. Also, both precision and sensitivity were similar for bins B and C using the global model, and the F1 score was around 0.8 for bin D and below >0.15 for Bins A-C. With the in-house model, the precision for low solubility compounds was 0.77 and for high solubility it was 0.91. The sensitivity was 0.70 for low solubility compounds but only 0.12 for high solubility compounds with the in-house model. Also, the F-score was high (0.74) for low solubility compounds and low for high solubility compounds (0.21). A total of 32% were correctly predicted with the category boundaries chosen. When using the global model for the same test set, only 7% of the poorly soluble compounds but 93% of the highly soluble

compounds were correctly predicted. Thus, 59% of all test compounds were correctly predicted (Table 3).

Predictions of metabolic stability in human liver microsomes

The AP global CYP_HLM_Clint model is based on the unbound concentrations, and these values were therefore converted to total CL_{int} (see Materials and Methods) to compare with the measured values for total CL_{int}. The total number of compounds with measured HLM CL_{int} was 4794. The measured CL_{int} values were divided into 4 categories, A-D (<15, 15-30, 30-80 and >80 $\mu\text{L}/\text{min}/\text{mg}$) and the same categories were used for binning the predictions. A 4 \times 4 confusion table was constructed. Around 40% (i.e., 1923 compounds) of the total number of compounds had a measured CL_{int} value >80 $\mu\text{L}/\text{min}/\text{mg}$ (bin D) and 28% (i.e., 1332 compounds) had a low CL_{int} value, category A (Table 1). Of the 1332 compounds measured to be stable (CL_{int} < 15 $\mu\text{L}/\text{min}/\text{mg}$), 40% were correctly predicted (Figure 4A). Of the 973 compounds (20% of all compounds) with a predicted CL_{int} <15 $\mu\text{L}/\text{min}/\text{mg}$, 55% were also stable when measured, while around 18% of the compounds were measured to be unstable (i.e., CL_{int} >80 $\mu\text{L}/\text{min}/\text{mg}$) in the assay. Overall, 37% of all compounds were correctly predicted (Table 3).

A training set consisting of 3595 of the compounds was used to build an in-house, local metabolic stability model, which was evaluated using the remaining 1199 compounds (i.e., the test set). Of the 340 compounds with measured high stability, 59% were correctly predicted (Figure 4B). 87% of the compounds with a predicted CL_{int} >80 $\mu\text{L}/\text{min}/\text{mg}$ had a measured value in the same range. Of the compounds with a predicted low CL_{int} (i.e., <15 $\mu\text{L}/\text{min}/\text{mg}$), 85% had a measured low CL_{int}, and less than 0.5% had a measured CL_{int} >80 $\mu\text{L}/\text{min}/\text{mg}$. Overall, 64% of the compounds in the test set were correctly predicted. When using the global AP model for predictions with the same test set, 37% of the compounds were

correctly predicted (Table 3 and Figure 4C). The prediction success is summarized in Table 2, demonstrating that the in-house model had a higher R^2 value (i.e., 0.71) than the global model (i.e., around 0.5 regardless if using all compounds or the test set).

The CYP_HLM_Clint model and the in-house CL_{int} model were also used to predict CL_{int} for a set of commercially available compounds with in-house measured data (the results are listed in Supplemental Table 2). The prediction success is shown in Table 4, demonstrating that the in-house model had a higher R^2 value (i.e., 0.51) than the global model (i.e., 0.14).

Permeability

The total number of compounds with measured Caco-2 P_{app} was 2586. Since the main AP software does not have a Caco-2 model, permeabilities were predicted with the global AP S+Peff model and compared with the measured Caco-2 values. The Membrane PlusTM or GastroPlusTM software, both from Simulations Plus, could be used to predict P_{app} values. We did not have access to these in this study. The local Caco-2 P_{app} model was built in the AP Modeler module using inhouse P_{app} data only.

When using all the compounds, 72% of the compounds with a measured P_{app} value of $\leq 2 \times 10^{-6}$ cm/s had a predicted P_{eff} value of $< 1 \times 10^4$ cm/s as shown in Figure 5A and Table 3. Of the compounds with a predicted human effective permeability in jejunum, S+Peff, of $< 1 \times 10^4$ cm/s, 64% demonstrated a measured apparent permeability in Caco-2, P_{app} , of $\leq 2 \times 10^{-6}$ cm/s (Table 3). 43% of the compounds were correctly predicted using the AP P_{eff} model and these categories.

A training set consisting of 2070 compounds was used to build an in-house, Caco-2 P_{app} model, which was evaluated using the remaining 516 compounds. Table 2 summarizes the statistics for the linear regression for the plot of predicted versus measured Caco-2 P_{app} based

on logarithmic data. The R^2 value was 0.61 for the in-house model (a R^2 value for the global model could not be obtained since the global model provides a P_{eff} value). 89% of the compounds in the test set with a predicted $P_{\text{app}} \leq 2 \times 10^{-6}$ cm/s had a measured value in the same range (Table 3). Of the compounds with a predicted high P_{app} (i.e., $>10 \times 10^{-6}$ cm/s), 69% also had a measured high P_{app} . The in-house model predicted 61 % of the test set correctly. When the global P_{eff} model was used to predict Caco-2 P_{app} categories for the test set, 47% were correctly predicted based on the bin categorisation. The sensitivity with both models was around 0.7 for low permeability compounds but lower for high permeability compounds.

The in-house model was also used to predict P_{app} for a set of commercially available reference compounds with in-house measured data (Supplemental Table 3). Table 4 shows that the R^2 for the regression (based on logarithmic data) was 0.78 (See Supplemental Table 4 for analysis of variance).

The prediction of P-gp substrates was also investigated. Predicted P-gp substrate (“yes”) was compared with a +/- P-gp inhibitor ratio of >1.5 in the Caco-2 assay, and with an ABBA ratio of >2.0 (Table 5). The precision, sensitivity, specificity and accuracy of these predictions were 75%, 96%, 30% and 75%, respectively when compared with the P-gp inhibitor ratio, and 93%, 92%, 14% and 82%, respectively, when compared with the ABBA ratio.

9. Discussion.

In the present study, the evaluations of the global ADME Predictor™ (AP) models for LogD, water solubility, metabolic stability in HLM and intestinal permeability were performed with experimental data from a total of 4794 Medivir compounds (not all compounds had measured data for all parameters). Also, in-house local models were built by using artificial neural network (ANN) models in the optional Modeler™ module of AP. For each parameter, approximately 75-80% of the Medivir data was used as a training set and the remaining compounds were used as a test set. With the global model, the test set and total dataset for each parameter gave similar precision and sensitivity, indicating that the test sets were representative.

Of the AP global models tested in this study, the S+LogD model demonstrated the best agreement with observed data (Table 2). This is likely explained by good agreement in assay output across laboratories, since the assay setup for the octanol-water partition assay is straightforward and not dependent on any biological test systems. The prediction success was somewhat better with the in-house local LogD model compared to the global model (Table 2).

Solubility is an important parameter for the bioavailability of drugs. Different methods are used for measuring solubility, e.g., thermodynamic solubility, kinetic solubility and dried DMSO solubility (Alelyunas et al., 2009; Saal and Petereit, 2012). Predictions of solubility are challenging since it is difficult to obtain consistent data for model building. In this work we used a set of in-house data obtained with a kinetic solubility assay performed at pH 7.4, based on 10 mM compounds in DMSO stock solutions, relevant for most early screening assays where compounds with solubility values below 10 μ M may precipitate. Unless high therapeutic concentrations will be needed, solubilities $>90 \mu$ M should be sufficient for preclinical assays and studies (even though high doses in safety studies in vivo may still be challenging). However, this solubility will not be relevant for other formulations in later

phases. Our data set was unbalanced, with a majority of compounds having high solubility. Only a small proportion (<3%) predicted solubility below 10 μ M using the global model, even though the dataset contained 21% compounds with low solubility. Moreover, most compounds with a low measured solubility had a high predicted solubility value using the global AP model. Thus, the S+S_{pH} (at pH 7.4) model was not very useful for filtering out the poorly soluble compounds for in vitro DMPK for the Medivir dataset. However, approximately 56% of the compounds were still predicted correctly, due to the large proportion of compounds with high solubility.

The prediction success for low solubility compounds was improved when the in-house local model was used. The global model overpredicted solubility and the in-house local model was better at identifying the low solubility compounds which could cause assay problems but underpredicted highly soluble compounds (see F1-scores, Table 3). However, with a majority of compounds having high solubility, the total number of correctly predicted compounds was lower for the in-house model than for the global model (Figure 3B and weighted F1 in Table 3).

Later in drug development it will be important with more accurate solubility measurements in relevant formulations and biological matrices. In AP, the solubility can be predicted at different pHs and also in some biologically relevant matrices such as FaSSGF, FaSSIF and FeSSIF which, if low, can help to explain one major reason for poor oral bioavailability in vivo.

Early screening of metabolic stability in HLM is routinely performed in drug discovery, since the metabolism of a compound will affect its overall pharmacokinetics (Sohlenius-Sternbeck et al., 2016). The prediction success for high and low CL_{int} compounds was increased when the in-house local model was used. However, none of the prediction models

predicted CL_{int} accurately in the range between low and high metabolic stability and do not give a reliable CL_{int} value for scaling to in vivo but the models can be useful for categorization of high and low metabolic stability. Predicted values in the range 15 to 30 $\mu\text{L}/\text{min}/\text{mg}$ often had measured values $<15 \mu\text{L}/\text{min}/\text{mg}$ (Figures 4A and B). This information could still be useful for most early projects, when trying to design metabolically stable compounds.

The AP and in-house models for metabolic stability were also tested with a set of reference compounds. These are commercially available compounds and may have been part of the training dataset for the AP global model. Nevertheless, the prediction outcome demonstrated higher R^2 for the in-house model compared to the AP model (Table 4), even though the structures for the in-house training set was dissimilar to the reference compounds. This may be due to experimental assay conditions being the same for the reference compounds and the in-house compounds in the training set, while the data for the training set in the AP global model may have come from several different experimental setups.

Intestinal permeability measurements are important for the understanding of absorption and bioavailability of oral drugs. The Caco-2 cell line is commonly used to measure apparent intestinal permeability and to give an indication of human absorption (Artursson et al., 2001). However, the permeability in Caco-2 cells is highly dependent on the experimental conditions (Hayeshi, 2008). There was no Caco-2 model available in the main AP software. However, Simulations Plus has prediction models in GastroPlusTM and Membrane PlusTM. In this work we used the global AP P_{eff} model to predict measured Caco-2 P_{app} values. Predicted P_{eff} values of 1 and 3.0×10^{-4} cm/s could be used as cut-offs for low and high permeability respectively. However, it is difficult to use predicted values between 1 and 3.0×10^{-4} cm/s to convert to specific Caco-2 P_{app} values or to predict the absolute absorption in vivo for moderate values. In early discovery, the model could still be used to indicate very low and high permeability

compounds. The in-house P_{app} model showed improved predictions for the test set, compared to the AP P_{eff} model, for low permeabilities (Table 3). The global model showed somewhat lower precision for low permeability compounds. Both the global P_{eff} model and the in-house P_{app} model could be useful tools to identify structures with likely low permeability, for the Medivir compounds, and to guide design and synthesis of more permeable compounds.

The in-house model for permeability was also tested with a set of commercial reference compounds, demonstrating similar prediction outcome as for the Medivir dataset with an R^2 value of 0.73 (Table 4).

The AP model for P-gp substrate identification was evaluated based on measured values of effect of P-gp inhibition and efflux ratio in ABBA. The P-gp model identified a large proportion of the compounds that were also shown to be P-gp substrates in the in vitro assays, giving high sensitivity and accuracy in confusion tables (see Table 5). However, chemical series with compounds that were P-gp substrates were overrepresented in the study (68%), and the reason for the low specificity number can be explained by the low number of negative data in the dataset.

Our evaluation shows that the global AP models can be used for rough categorization of high and low values in early discovery, based on predicted results for metabolic stability in HLM and P_{eff} permeability, and to give accurate predictions of Log D, guiding the synthesis of new compounds and for prioritizing in vitro ADME experiments. The model seems to overpredict solubility for Medivir compounds, however. It can be useful to also look at pH- and matrix-dependent solubility models in AP. Local in-house prediction models built with the optional AP Modeler Module can improve predictions. As more data is generated, the in-house models will likely have to be rebuilt, when structures move away from the initial training set.

Predictions of advantageous ADME properties should trigger further experimental evaluations. There is often a trade off with efficacy and toxicity so, if in vitro efficacy is promising, selected compounds with poor predicted properties should be experimentally tested in ADMET assays to confirm the predictions and be balanced against potency, toxicity, predicted dose and dosing regimen. Depending on the specific project criteria, such as indication, dose and intended dosing regimen, a project can, of course, accept compounds with some poor properties.

10. Acknowledgement.

We thank Dr Fredrik Öberg, Chief Scientific Officer at Medivir AB, for allowing us to use these data.

11. Authorship Contributions.

Participated in research design: Sohlenius-Sternbeck, Terelius

Performed data analysis: Sohlenius-Sternbeck, Terelius

Wrote the manuscript: Sohlenius-Sternbeck, Terelius

Financial disclosure: No author has an actual or perceived conflict of interest with the contents of this article.

12. Referenses

- Alelyunas YW, Liu R, Pelosi-Kilby L, and Shen, C (2009) Application of a Dried-DMSO rapid throughput 24-h equilibrium solubility in advancing discovery candidates. *Eur J Pharm Sci* **37**: 172–182.
- Alqahtani S (2017) In silico ADME-Tox modeling: progress and prospects. *Expert Opin Drug Metab Toxicol* **13**: 1147–1158.
- Artursson P, Palm K, and Luthman K (2001) Caco-2 monolayers in experimental and theoretical predictions of drug transport. *Adv Drug Deliv Rev* **46**: 27-43.
- Austin RP, Barton P, Cockcroft SL, Wenlock MC, and Riley RJ (2002) The influence of nonspecific microsomal binding on apparent intrinsic clearance, and its prediction from physicochemical properties. *Drug Metab Dispos* **30**: 1497-1503.
- Ballard P, Brassil P, Bui KH, Dolgos H, Petersson C, Tunek A, and Webborn PJH (2012) The right compound in the right assay at the right time: an integrated discovery DMPK strategy. *Drug Metab Rev* **44**: 224-252.
- Giacomini KM, Huang SM, Tweedie DJ, Benet LZ, Brouwer KL, Chu X, Dahlin A, Evers R, Fischer V, Hillgren KM, Hoffmaster KA, Ishikawa T, Keppler D, Kim RB, Lee CA, Niemi M, Polli JW, Sugiyama Y, Swaan PW, Ware JA, Wright SH, Yee SW, Zamek-Gliszczynski MJ, and Zhang L (2010). Membrane transporters in drug development. *Nat Rev Drug Discov* **9**: 215-236.
- Gleeson MP, and Montanari D (2012) Strategies for the generation, validation and application of in silico ADMET models in lead generation and optimization. *Expert Opin on Drug Metab Toxicol* **8**: 1435-1446.
- Hayeshi R, Hilgendorf C, Artursson P, Augustijns P, Brodin B, Dehertogh P, Fisher K, Fossati L, Hovenkamp E, Korjamo T, Masungi C, Maubon N, Mols R, Müllertz A, Mönkkönen J, O’Driscoll C, Oppers-Tiemissen HM, Ragnarsson EGE, Rooseboom M, and Ugnell AL. Comparison of drug transporter gene expression and functionality in Caco-2 cells from 10 different laboratories (2008) *Eur J of Pharm Sci* **35**: 383–396.

- Kramer JA, Sagartz JE and Morris DL (2007) The application of discovery toxicology and pathology towards the design of safer pharmaceutical lead candidates. *Nat Rev Drug Discov* **6**: 636–649.
- Liu R, Schyman P, and Wallqvist A (2015) Critically assessing the predictive power of QSAR models for human liver microsomal stability. *J Chem Inf Model* **55**: 1566–1575.
- Kazmi SR, Jun R, Yu M-S, Jung C, and Na D (2019) In silico approaches and tools for the prediction of drug metabolism and fate: A review. *Comput Biol Med* **106**: 54–64.
- Moda TL, Torres LG, Carrara AE, and Andricopulo AD (2008) PK/DB: database for pharmacokinetic properties and predictive. *Bioinformatics* **24**: 2270–2271.
- Saal C, and Peterleit AC (2012) Optimizing solubility: Kinetic versus thermodynamic solubility temptations. *Eur J Pharm Sci* **47**: 589–595.
- Sohlenius-Sternbeck AK, Afzelius L, Prusis P, Neelissen J, Hoogstraate J, Johansson J, Floby E, Bengtsson A, Gissberg O, Sternbeck J, and Petersson C (2010) Evaluation of the human prediction of clearance from hepatocyte and microsome intrinsic clearance for 52 drug compounds. *Xenobiotica* **40**: 637–649.
- Sohlenius-Sternbeck AK, Janson J, Bylund J, Baranczewski P, Breitholtz-Emanuelsson A, Hu Y, Tsoi C, Lindgren A, Gissberg O, Bueters T, Briem S, Juric S, Johansson J, Bergh M, and Hoogstraate J (2016) Optimizing DMPK Properties: Experiences from a Big Pharma DMPK Department. *Curr Drug Metab* **17**: 253–270.
- Sohlenius-Sternbeck AK, Meyerson G, Hagbjörk AL, Juric S, and Terelius Y (2018) A strategy for early-risk predictions of clinical drug-drug interactions involving the GastroPlus™ DDI module for time-dependent CYP inhibitors. *Xenobiotica* **48**: 348–356.
- Stålring J, Sohlenius-Sternbeck AK, Terelius Y, and Parkes K (2018) Confident application of a global human liver microsomal activity QSAR. *Future Med Chem* **10**: 1575–1588.
- Wang Y, Xing J, Xu Y, Zhou N, Peng J, Xiong Z, Liu X, Luo X, Luo C, Chen K, Zheng M, and Jiang H (2015) In silico ADME/T modelling for rational. *Q Rev Biophys* **48**: 488–515.
- van de Waterbeemd H, and Gifford E (2003) ADMET in silico modelling: Towards prediction paradise? *Nat Rev Drug Discov* **2**: 192–204.

Yan A, and Gasteiger J (2003) Prediction of Aqueous Solubility of Organic Compounds by Topological Descriptors. *QSAR Comb Sci* **22**: 821-829.

13. Footnotes

This work received no external funding.

14. Figure Legends.

Figure 1. Characteristics of the Medivir dataset (4794 compounds) demonstrated by histograms showing A) the distribution of molecular weight, and B) the distribution of measured LogD (1198 compounds),

Figure 2. Predicted LogD versus measured LogD using A) the global S+LogD model (AP model) for all 1198 compounds with measured values, B) the in-house (local) model for the test set (287 compounds), and C) the S+LogD model for the test set.

Figure 3. Predicted solubility versus measured solubility in 4 categories using A) the global S+S_{pH} model at pH 7.4 (AP model) for all 2778 compounds with measured values, B) the in-house (local) model for the test set (691 compounds), and C) the global S+S_{pH} model for the test set. For each bin, the number of compounds with predicted solubility in the specified range is presented as percentage of total compounds in the bin. Note that for the S+S_{pH} model the solubility was converted from mg/ml to μM .

Figure 4. Predicted CL_{int} versus measured CL_{int} in 4 categories using A) the global CYP_HLM_Clint model (AP model), versus measured total HLM CL_{int} for all 4794 compounds with measured values, B) the in-house (local) model for the test set (1199 compounds), and C) the global CYP_HLM_Clint model for the test set. For each bin, the number of compounds with predicted CL_{int} in the specified range is presented as percentage of total compounds in the bin. Note that the predicted CL_{int} from the CYP_HLM_Clint was converted to total CL_{int} using the predicted S+ $f_{\text{u}_{\text{mic}}}$ (global AP model).

Figure 5. Predicted intestinal permeability (P_{eff} or P_{app}) versus measured Caco-2 P_{app} in 4 categories using A) the S+Peff model (AP model) for all 2586 compounds with measured P_{app} values, and B) the in-house (local) model for the test set (516 compounds), and C) the S+Peff model for the test set. For each bin, the number of compounds with predicted P_{eff} or P_{app} in the specified range is presented as percentage of total compounds in the bin.

15. Tables.

Table 1. Bin size for the datasets. The measured solubilities were divided into 4 categories, A-D (<10, 10-50, 50-90 and >90 μM) and the same categories were used for binning the predictions. The measured CL_{int} values were divided into 4 categories, A-D (<15, 15-30, 30-80 and >80 $\mu\text{L}/\text{min}/\text{mg}$) and the same categories were used for binning the predictions. The measured P_{app} values were divided into 4 categories, A-D (<2, 2-5, 5-10 and >10 $\times 10^{-6}$ cm/s) and the corresponding categories A-D used for P_{eff} predictions were <1, 1-2, 2-3 and >3 (10^{-4} cm/s).

| Parameter predicted | Model | Data-set | Tot cpds | Tot correctly predicted | Predicted bin size | | | | Measured bin size | | | |
|---|--------------------------------|----------|----------|-------------------------|--------------------|-------|-------|-------|-------------------|-------|-------|-------|
| | | | | | Bin A | Bin B | Bin C | Bin D | Bin A | Bin B | Bin C | Bin D |
| Solubility (μM) | AP | All | 2778 | 1553 | 69 | 241 | 201 | 2267 | 582 | 319 | 340 | 1537 |
| | AP | Test | 691 | 410 | 13 | 46 | 47 | 585 | 101 | 78 | 92 | 420 |
| | local | Test | 691 | 221 | 92 | 140 | 404 | 55 | 101 | 78 | 92 | 420 |
| Metabolic stability HLM CL_{int} ($\mu\text{L}/\text{mg}/\text{min}$) | AP | All | 4794 | 1779 | 973 | 1586 | 1444 | 791 | 1332 | 598 | 941 | 1923 |
| | AP | Test | 1199 | 442 | 231 | 385 | 382 | 201 | 340 | 135 | 232 | 492 |
| | local | Test | 1199 | 766 | 235 | 236 | 309 | 419 | 340 | 135 | 232 | 492 |
| Permeability Caco-2 P_{app} (10^{-6} cm/s) | AP, P_{eff} | All | 2586 | 1114 | 1072 | 856 | 341 | 317 | 962 | 306 | 399 | 919 |
| | AP, P_{eff} | Test | 516 | 245 | 220 | 154 | 72 | 70 | 204 | 61 | 78 | 173 |
| | local, P_{app} | Test | 516 | 317 | 166 | 90 | 87 | 173 | 204 | 61 | 78 | 173 |

AP = ADMET PredictorTM; CL_{int} = in vitro intrinsic clearance; P_{eff} = effective jejunal permeability; P_{app} = apparent permeability

Table 2. Prediction outcome for the AP models and the in-house models for compounds in the Medivir dataset.

| Assay | Total number of compounds | Number of compounds in training set | Number of compounds in test set | AP model (all compounds) | | | AP model (test set) | | | In-house model (test set) | | |
|------------------------------|---------------------------|-------------------------------------|---------------------------------|--------------------------|-------|----------------|---------------------|-------|----------------|---------------------------|-------|----------------|
| | | | | RMSE | MAE | R ² | RMSE | MAE | R ² | RMSE | MAE | R ² |
| LogD | 1198 | 911 | 287 | 0.771 | 0.589 | 0.785 | 0.757 | 0.585 | 0.790 | 0.488 | 0.349 | 0.888 |
| Solubility* | 2778 | 2087 | 691 | 1.261 | 1.075 | 0.260 | 1.229 | 1.055 | 0.202 | 0.388 | 0.247 | 0.593 |
| HLM CL_{int}* | 4794 | 3595 | 1199 | 0.566 | 0.454 | 0.531 | 0.574 | 0.482 | 0.498 | 0.327 | 0.250 | 0.717 |
| Caco-2 permeability* | 2586 | 2070 | 516 | NA | NA | NA | NA | NA | NA | 0.370 | 0.265 | 0.614 |

*Model based on logarithmic data

AP = ADMET PredictorTM; HLM = human liver microsomes; MAE = mean absolute error; RMSE = root mean square error

Table 3. Precision, sensitivity and F1-score for each bin as well as overall accuracy and weighted F1 for the global models with the total datasets and for the in-house and global models with the test sets.

The measured solubilities were divided into 4 categories, A-D (<10, 10-50, 50-90 and >90 μM) and the same categories were used for binning the predictions. The measured CL_{int} values were divided into 4 categories, A-D (<15, 15-30, 30-80 and >80 $\mu\text{L}/\text{min}/\text{mg}$) and the same categories were used for binning the predictions. The measured P_{app} values were divided into 4 categories, A-D (≤ 2 , 2-5, 5-10 and $>10 \times 10^{-6}$ cm/s) and the corresponding categories A-D used for P_{eff} predictions were <1, 1-2, 2-3 and >3 (10^{-4} cm/s).

| Parameter predicted | Model | Data-set | Tot cpds | Accuracy (Tot correct) in % | Precision (Predictive value) or Predicted bin, correct prediction | | | | Sensitivity or recall Measured bin, correctly predicted | | | | F1-score | | | | Weighted F1 |
|---|--------------------------------|----------|----------|-----------------------------|---|-------|-------|-------|---|-------|-------|-------|----------|-------|-------|-------|-------------|
| | | | | | Bin A | Bin B | Bin C | Bin D | Bin A | Bin B | Bin C | Bin D | Bin A | Bin B | Bin C | Bin D | |
| | | | | | Solubility (μM) | AP | All | 2778 | 56 | 0.68 | 0.14 | 0.11 | 0.64 | 0.08 | 0.10 | 0.06 | |
| AP | test | 691 | 59 | 0.54 | | 0.09 | 0.15 | 0.67 | 0.07 | 0.05 | 0.08 | 0.95 | 0.12 | 0.06 | 0.10 | 0.78 | 0.51 |
| local | test | 691 | 32 | 0.77 | | 0.29 | 0.15 | 0.91 | 0.70 | 0.51 | 0.65 | 0.11 | 0.74 | 0.37 | 0.24 | 0.21 | 0.31 |
| Metabolic Stability HLM CL_{int} ($\mu\text{L}/\text{mg}/\text{min}$) | AP | All | 4794 | 37 | 0.55 | 0.16 | 0.26 | 0.79 | 0.40 | 0.42 | 0.40 | 0.33 | 0.46 | 0.23 | 0.31 | 0.46 | 0.40 |
| | AP | test | 1199 | 37 | 0.54 | 0.16 | 0.26 | 0.78 | 0.36 | 0.47 | 0.42 | 0.33 | 0.43 | 0.24 | 0.32 | 0.45 | 0.40 |
| | local | test | 1199 | 64 | 0.85 | 0.28 | 0.43 | 0.87 | 0.59 | 0.50 | 0.58 | 0.74 | 0.70 | 0.36 | 0.50 | 0.80 | 0.66 |
| Permeability Caco-2 P_{app} (10-6 cm/s) | AP, P_{eff} | All | 2586 | 43 | 0.64 | 0.16 | 0.18 | 0.72 | 0.72 | 0.44 | 0.16 | 0.25 | 0.68 | 0.23 | 0.17 | 0.37 | 0.44 |
| | AP, P_{eff} | test | 516 | 47 | 0.68 | 0.19 | 0.24 | 0.69 | 0.74 | 0.49 | 0.22 | 0.28 | 0.71 | 0.28 | 0.23 | 0.40 | 0.48 |
| | local, P_{app} | test | 516 | 61 | 0.89 | 0.30 | 0.25 | 0.69 | 0.73 | 0.44 | 0.28 | 0.69 | 0.80 | 0.36 | 0.27 | 0.69 | 0.63 |

AP = ADMET PredictorTM; CL_{int} = in vitro intrinsic clearance; HLM = human liver microsomes; P_{eff} = effective jejunal permeability; P_{app} = apparent permeability

Table 4. Prediction outcome for CL_{int} in HLM and Caco-2 with the AP models and the in-house models for commercially available reference compounds with in-house measured data (See Supplemental Tables 2 and 3).

| Assay | Number of compounds | AP model | | | In-house model | | |
|-----------------------------------|---------------------|----------|-------|----------------|----------------|-------|----------------|
| | | RMSE | MAE | R ² | RMSE | MAE | R ² |
| Human liver microsomal CL_{int} | 75 | 0.454 | 0.333 | 0.140 | 0.313 | 0.247 | 0.512 |
| Caco-2 permeability | 26 | NA | NA | NA | 0.333 | 0.265 | 0.782 |

Analysis based on logarithmic data.

NA: Not available since the ADMET PredictorTM (AP) model predicted effective jejunal permeability (P_{eff}), not apparent permeability (P_{app})

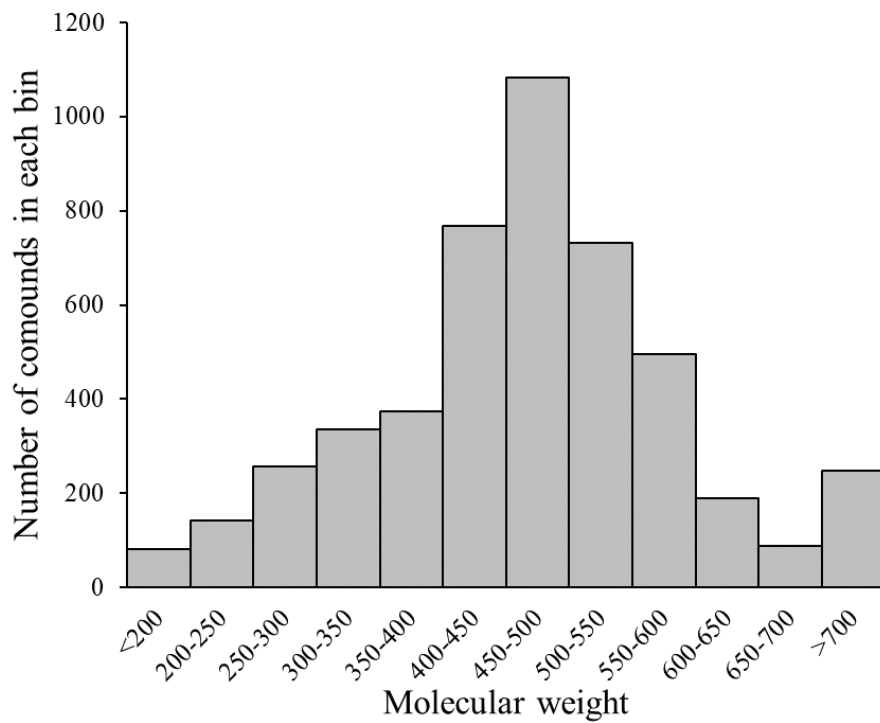
Table 5. Confusion tables demonstrating AP performance in predicting P-gp substrates for the 387 Medivir compounds tested in the P-gp inhibitor assay and in predicting P-gp substrates for the 103 Medivir compounds tested in the ABBA assay. Predicted P-gp substrate (“yes”) was compared with a measured + P-gp inhibitor/- P-gp inhibitor ratio of >1.5 and with an ABBA ratio of >2.0. The total number of compounds with a measured ratio >1.5 in the +P-gp inhibitor/-P-gp inhibitor assay was 264 (i.e. 68% of compounds tested), and the total number of compounds with a measured ratio >2 in the ABBA assay was 94 (i.e.91% of compounds tested).

| Caco-2 assay setup | TY | FY | TN | FN | Precision TY/(TY+FY) | Sensitivity TY/(TY+FN) | Specificity TN/(TN+FY) | Accuracy (TY+TN)/total |
|---------------------------|-----------|-----------|-----------|-----------|---------------------------------|-----------------------------------|-----------------------------------|-----------------------------------|
| +/- P-gp inhibitor | 254 | 86 | 37 | 10 | 0.75 | 0.96 | 0.30 | 0.75 |
| ABBA | 87 | 7 | 2 | 7 | 0.93 | 0.92 | 0.14 | 0.82 |

TY is predicted True “Yes”, TN is predicted True “No”, FY is predicted False “Yes” and FN is predicted False “No”; ABBA, apical to basolateral and basolateral to apical

Figure 1.

A)



B)

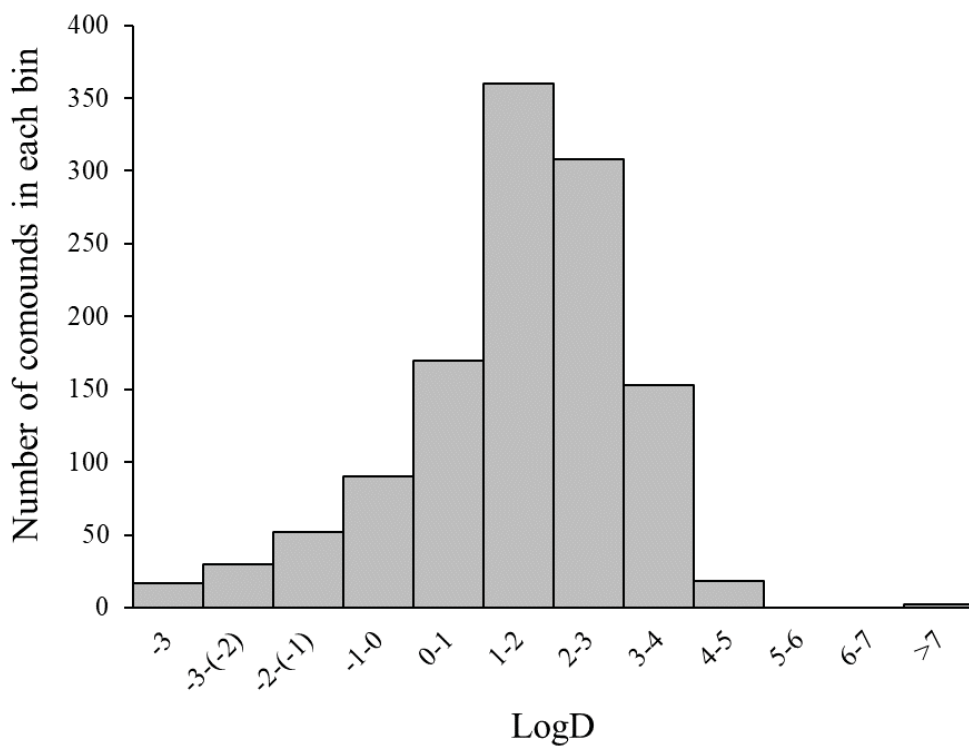
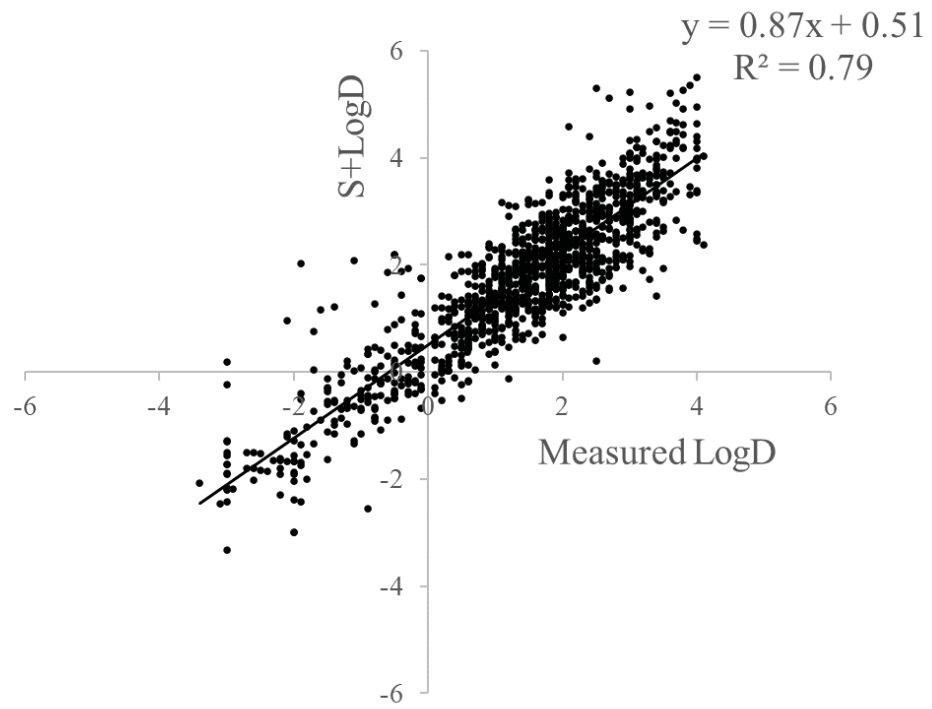
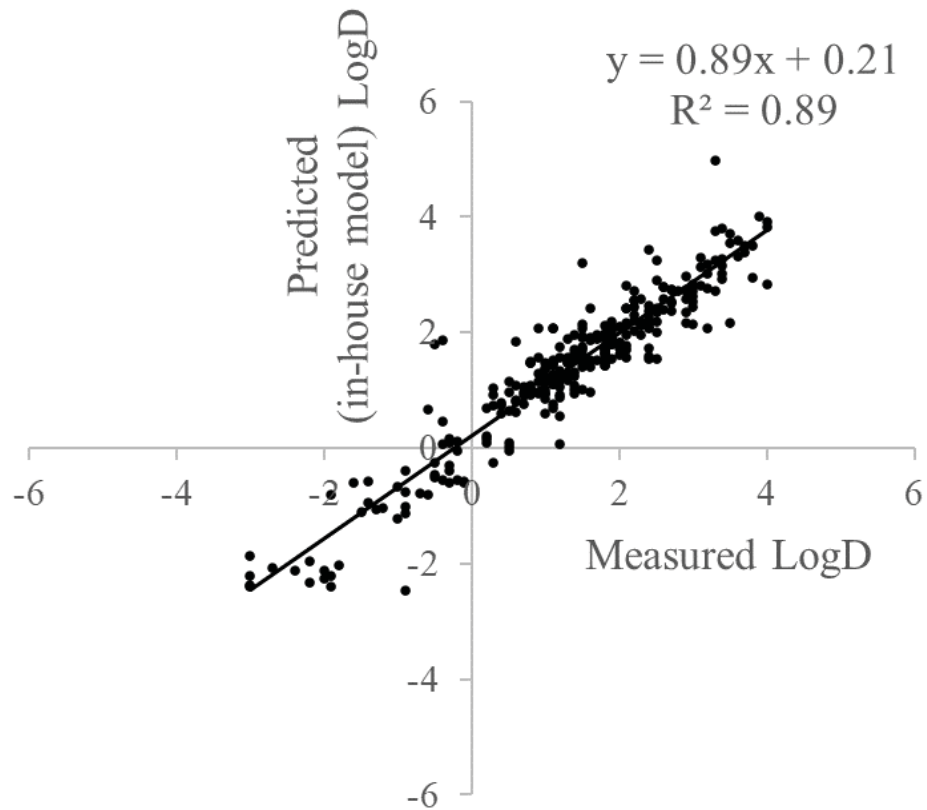


Figure 2.

A)



B)



c)

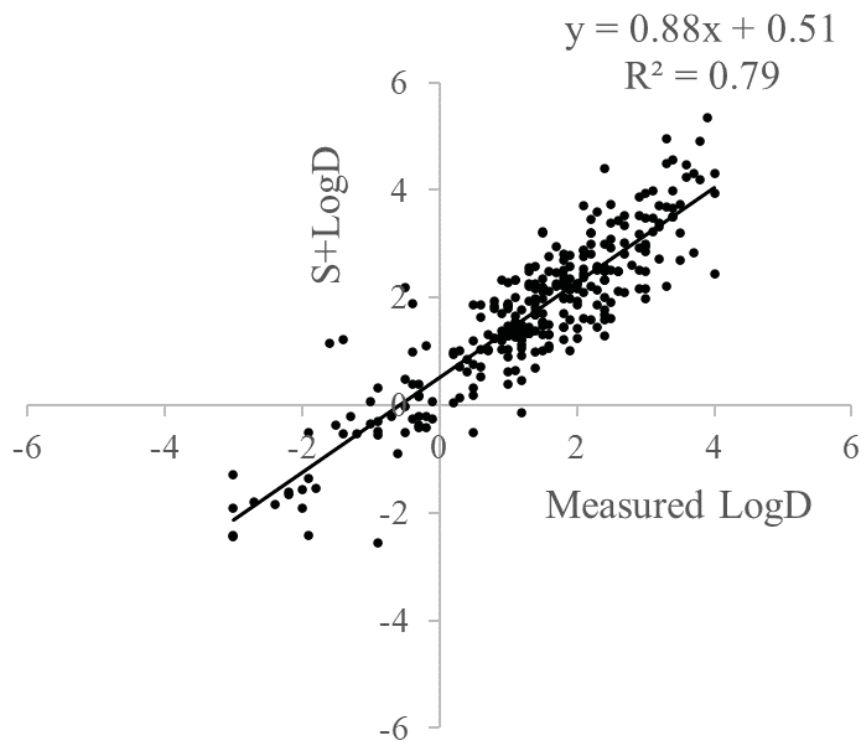
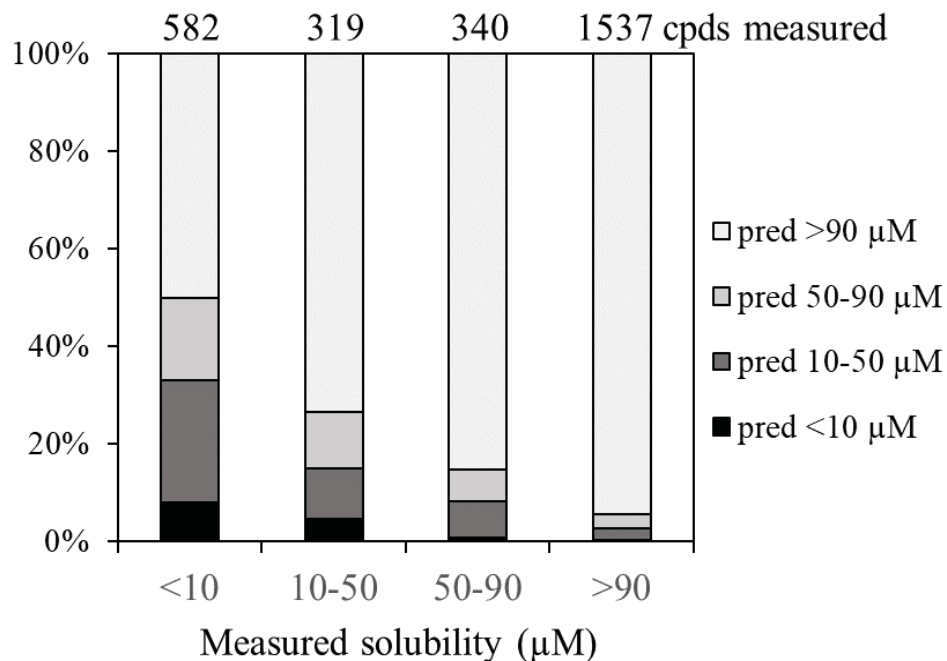


Figure 3.

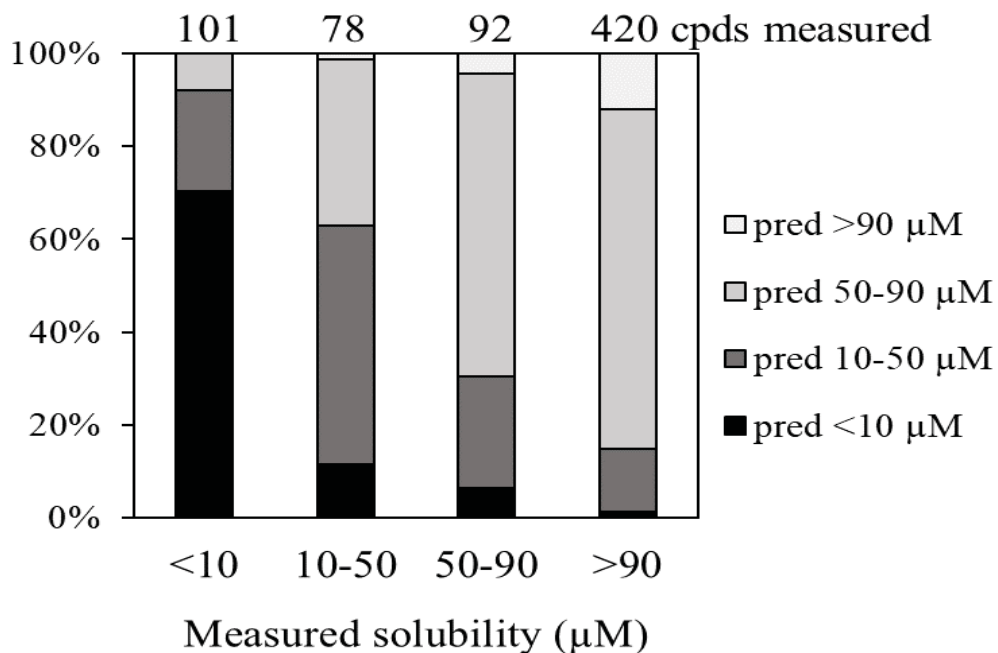
A)

**Predicted (AP model) vs measured solubility
in % of total number measured**



B)

**Predicted (in-house model) vs measured
solubility in % for test set (691 cpds)**



c)

Predicted (global AP model) vs measured solubility in % for the test set (691 cpds)

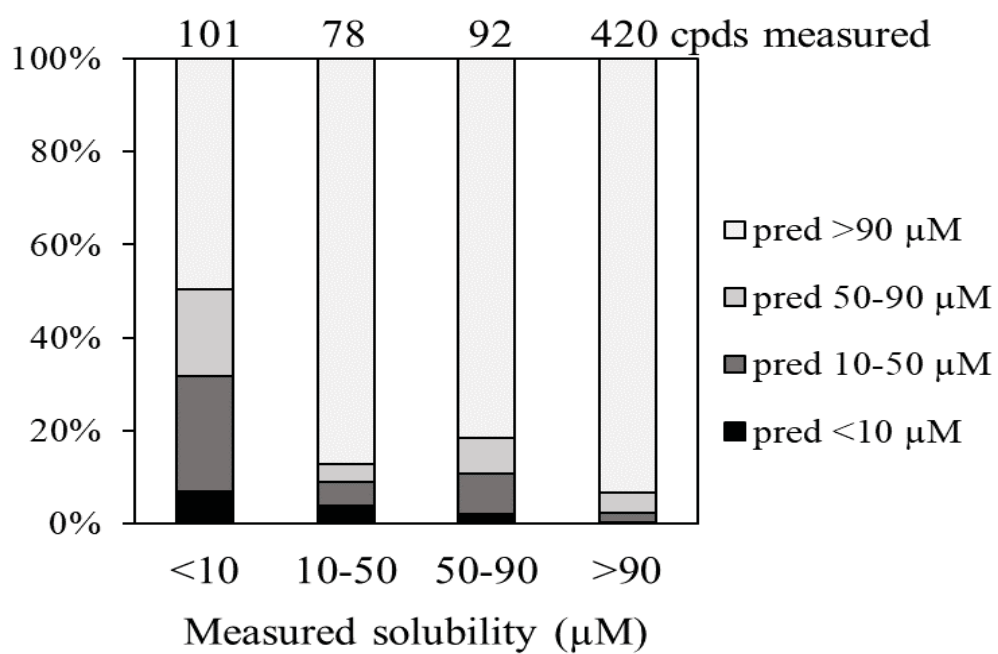
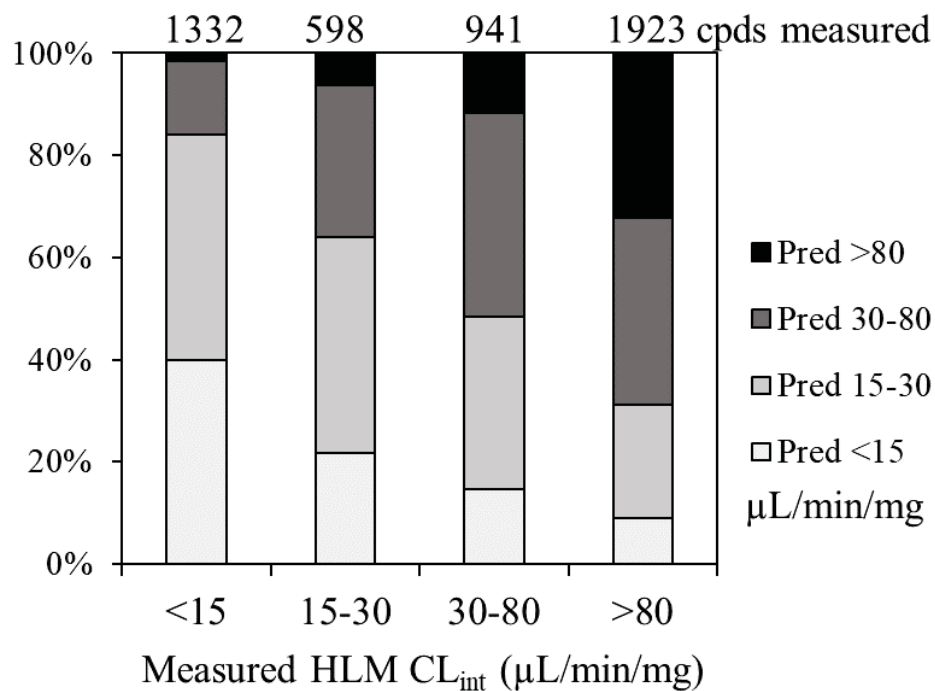


Figure 4.

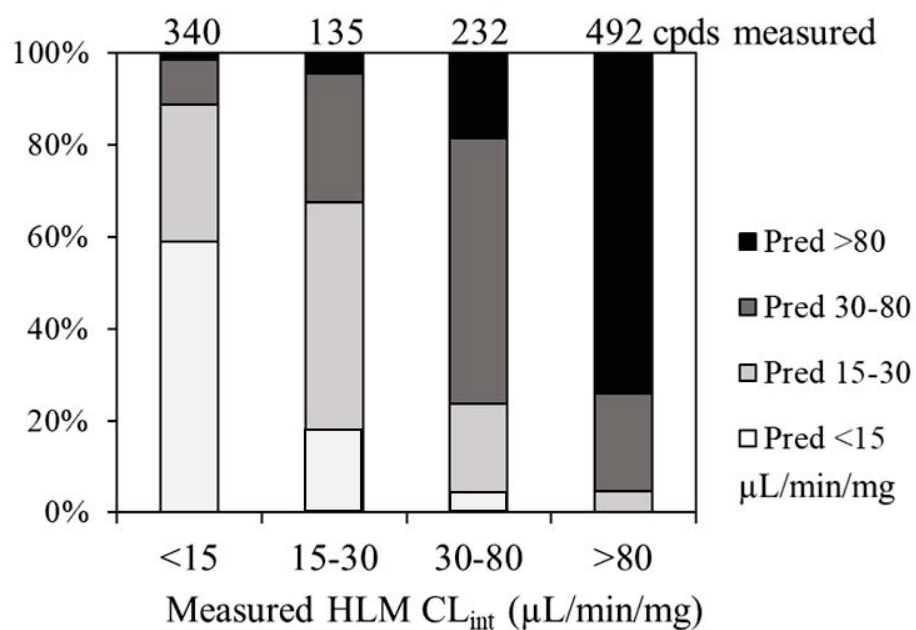
A)

Predicted (AP model) vs measured HLM tot CL_{int} in % for all 4794 compounds



B)

Predicted (local model) vs measured HLM tot CL_{int} in % for 1199 compounds in test set



C)

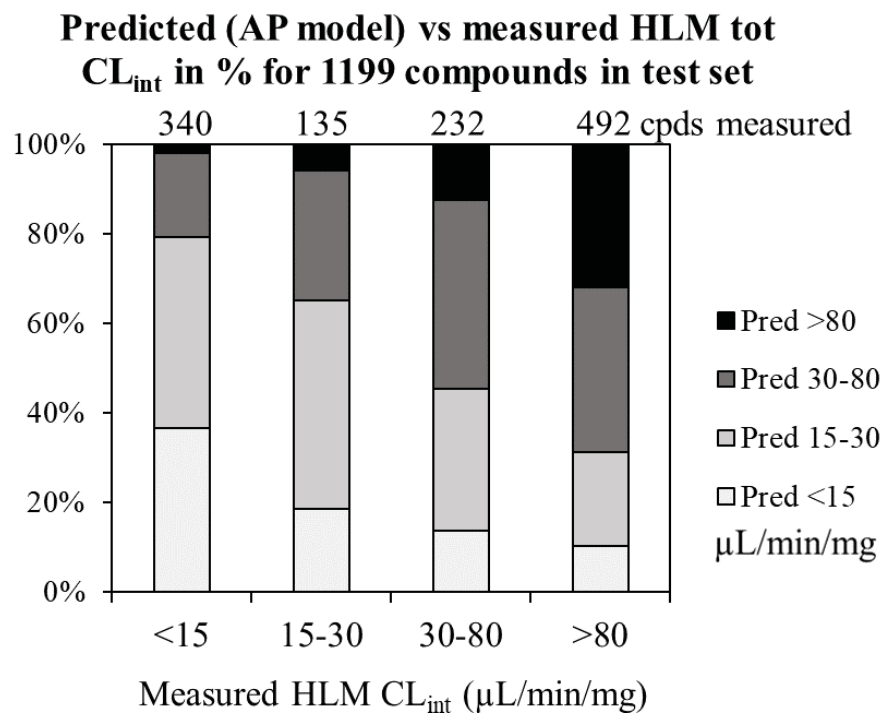
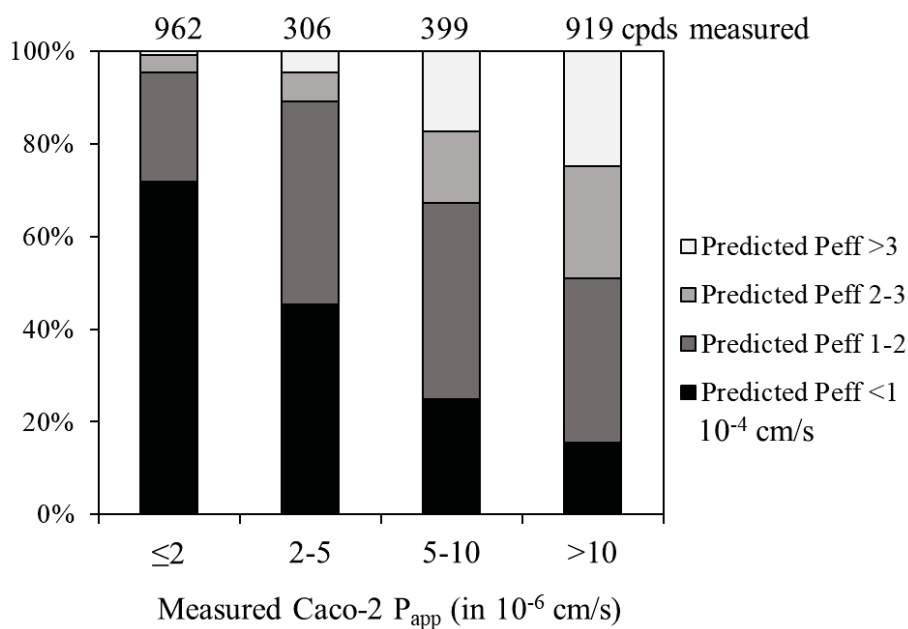


Figure 5.

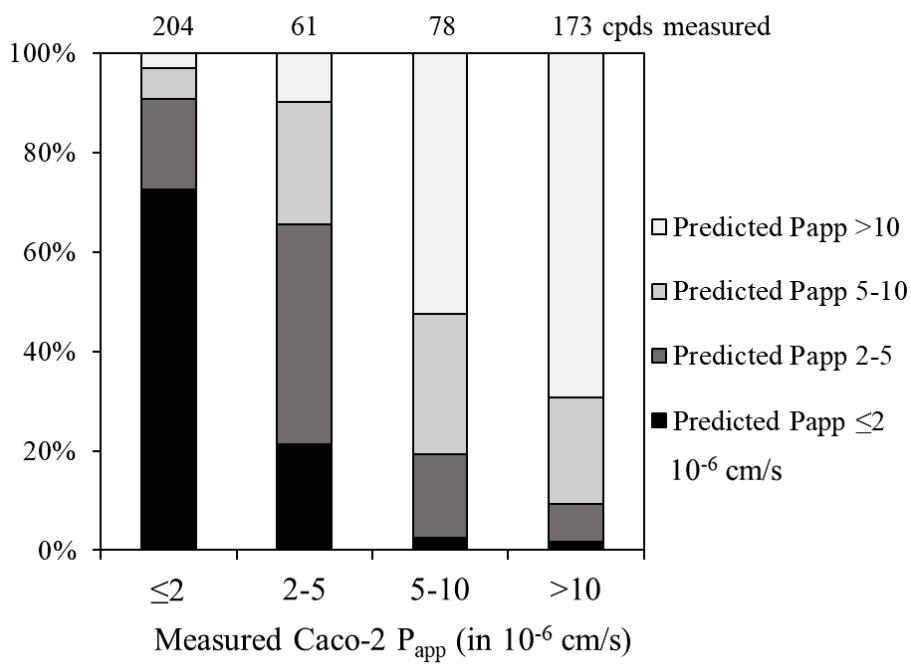
A)

Predicted P_{eff} (10^{-4} cm/s, AP model) vs measured Caco-2 P_{app} (10^{-6} cm/s) in % for all 2586 compounds

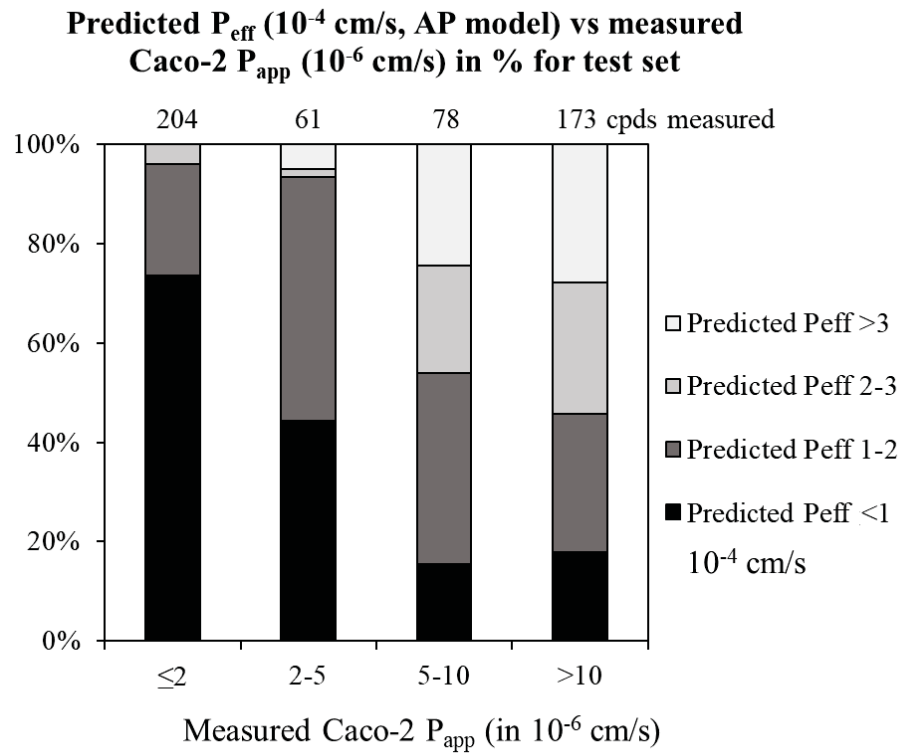


B)

Predicted vs measured Caco-2 P_{app} (10^{-6} cm/s) in % for 516 compounds in the test set, local model



C)



DATA SUPPLEMENTS

Evaluation of ADMET Predictor™ in early discovery DMPK project work

Anna-Karin Sohlenius-Sternbeck and Ylva Terelius

Drug Metabolism and Disposition

DMD-AR-2021-000552

Supplemental Table 1

The first data column in Supplemental Tables 1A-E summarizes quality control data for LogD, kinetic solubility, metabolic stability in HLM and permeability in Caco-2 cells. Criteria for rejecting an experiment is based on whether data is outside two standard deviations of the Manhattan mean. Only data from accepted experiments were used.

1A. Quality control reference data for LogD. The first data column shows the Manhattan mean \pm standard deviation from 12 separate experiments.

| Quality control reference compound | LogD | Acceptable LogD range in assay | Predicted LogD S+LogD model | In-house LogD model |
|------------------------------------|------------------|--------------------------------|-----------------------------|---------------------|
| Ketoconazole | 3.21 \pm 0.12 | 3.0-3.45 | 3.71 | 3.02 |
| Metoprolol | -0.36 \pm 0.07 | -0.5-(-0.2) | -0.128 | 0.03 |
| Propranolol | 1.04 \pm 0.07 | 0.9-1.2 | 0.949 | 1.09 |

1B. Quality control reference data for kinetic solubility. The first data column shows the Manhattan mean (\pm standard deviation for diethylstilbestrol) from 191 separate experiments.

| Quality control reference compound | Solubility (μ M) | Acceptable kinetic solubility range in assay | Predicted S+S_pH (μ M) | In-house solubility model (μ M) |
|------------------------------------|-----------------------|--|-----------------------------|--------------------------------------|
| Albendazole | <2 | <2 | 60 | 3.1 |
| Diethylstilbestrol | 7.7 \pm 1.6 | 4.5-11 | 89 | 53 |
| Flurbiprofen | >95 | >95 | 29074 | 73 |

1C. Quality control reference data for metabolic stability in human liver microsomes. The first data column shows the Manhattan mean \pm standard deviation from 26 in-house experiments. For predicted values see Supplemental Table 2.

| Quality control reference compound | CL _{int} (μ l/min/mg) | Acceptable CL _{int} range in assay (μ l/min/mg) |
|------------------------------------|-------------------------------------|---|
| Bufuralol | 20.6 \pm 2.4 | 16-25 |
| Diclofenac | 131 \pm 12.7 | 105-156 |
| Midazolam | >300 | >300 |
| Phenacetin | 10.0 \pm 2.3 | 5-15 |

CL_{int}, in vitro intrinsic clearance

1D. Quality control reference data for permeability in Caco-2 cells. The first data column shows the Manhattan mean \pm standard deviation from 62 separate experiments. For predicted values see Supplemental Table 3.

| Quality control reference compound | P_{app} (10^{-6} cm/s) | Acceptable P_{app} range in assay (10^{-6} cm/s) |
|------------------------------------|-----------------------------|---|
| Atenolol | <1 | <1 |
| Digoxin | 1.0 ± 0.6 | <2 |
| Digoxin + 5 μ M GF* | 6.0 ± 1.9 | NA |
| Propranolol | 17.9 ± 3.8 | 10-25 |

* In the presence of 5 μ M GF, a P-gp inhibitor, a 6-fold higher P_{app} was obtained.

NA = Not applicable

GF, GF120918 (Elacridar); P_{app} , apparent permeability

1E. Quality control reference data for permeability in the Caco-2 ABBA assay. The first data column shows the Manhattan mean \pm standard deviation from 15 separate experiments.

| Quality control reference compound | ABBA ratio | Acceptable ABBA ratio range | Predicted P-gp substrate AP model |
|------------------------------------|----------------|-----------------------------|-----------------------------------|
| Digoxin | 15.9 ± 3.8 | >2 | Yes |
| Quinidine | 3.2 ± 0.9 | >2 | Yes |

ABBA, apical to basolateral and basolateral to apical

Supplemental Table 2.

Measured total CL_{int} in HLM for a set of reference compounds and the predicted CL_{int} using the global AP model for unbound CL_{int} (CYP_HLM_Clint), converted to predicted total CL_{int} using the predicted unbound fraction, $S+fu$ from AP. The last column shows the CL_{int} predictions using the in-house CL_{int} model (built on measured total CL_{int} data). Data is the mean of at least three independent experiments.

| Compound | Measured total CL_{int} ($\mu\text{L}/\text{min}/\text{mg}$) | CYP_HLM_Clint converted to total CL_{int}($\mu\text{L}/\text{min}/\text{mg}$) | In-house HLM total CL_{int} model ($\mu\text{L}/\text{min}/\text{mg}$) |
|------------------|---|--|---|
| Abexinostat | 6.0 | 10.2 | 10.0 |
| Acetaminophen | 6.0 | 21.6 | 7.3 |
| Aliskiren | 20.0 | 13.1 | 54.4 |
| Amitriptyline | 83.0 | 18.0 | 18.7 |
| Antipyrine | 6.0 | 31.1 | 14.0 |
| Atazanavir | 100.0 | 110.8 | 110.0 |
| Atenolol | 2.8 | 2.5 | 6.6 |
| Belinostat | 19.0 | 13.2 | 12.7 |
| Betaxolol | 13.0 | 7.6 | 13.2 |
| Bosentan hydrate | 15.0 | 33.1 | 41.1 |
| Bufuralol | 20.6 | 10.0 | 19.5 |
| Bupropion | 6.0 | 15.5 | 19.7 |
| Caffeine | 17.0 | 15.8 | 5.7 |
| Carvedilol | 47.0 | 13.9 | 35.5 |
| Cerivastatin | 9.5 | 7.8 | 10.8 |
| Chlorpheniramine | 54.0 | 29.5 | 21.8 |
| Chlorpromazine | 45.0 | 38.2 | 50.5 |
| Cimetidine | 6.0 | 15.8 | 7.5 |
| Coumarin | 49.0 | 23.0 | 22.4 |
| Cyclopropavir | 7.0 | 9.0 | 5.8 |
| Degrasyn | 14.0 | 53.7 | 52.9 |
| Desipramine | 22.0 | 19.7 | 19.7 |
| Diazepam | 13.0 | 17.7 | 67.2 |
| Diclofenac | 131.0 | 11.7 | 14.5 |
| Diltiazem | 58.0 | 15.8 | 35.6 |
| Diphenhydramine | 39.0 | 19.2 | 12.9 |
| Dofetilide | 7.1 | 5.4 | 11.8 |
| Furafylline | 8.0 | 10.7 | 6.6 |
| Furosemide | 6.0 | 9.0 | 9.3 |
| Gemfibrozil | 29.0 | 8.3 | 22.3 |
| Glipizide | 29.0 | 24.8 | 13.0 |
| Granisetron | 6.0 | 8.2 | 9.1 |
| Ibudilast | 21.0 | 11.0 | 34.3 |
| Ibuprofen | 14.0 | 11.6 | 16.9 |

| | | | |
|-----------------|--------|-------|-------|
| Imipramine | 6.0 | 13.5 | 29.2 |
| Irbesartan | 14.0 | 16.0 | 20.1 |
| Ketoprofen | 13.0 | 11.7 | 11.2 |
| Lorcainide | 45.0 | 23.8 | 67.0 |
| Mepazine | 48.0 | 44.1 | 41.7 |
| Mephenytoin | 6.0 | 20.9 | 7.7 |
| Metoprolol | 6.0 | 5.8 | 9.7 |
| Midazolam | >300.0 | 50.0 | 77.3 |
| Nadolol | 8.1 | 6.6 | 8.2 |
| Naloxone | 10.0 | 8.7 | 15.3 |
| Naproxen | 11.0 | 9.6 | 10.4 |
| Ondansetron | 37.0 | 27.5 | 13.7 |
| Orphenadrine | 6.0 | 20.8 | 14.8 |
| Panobinostat | 8.0 | 7.5 | 7.9 |
| Paroxetine | 18.0 | 16.2 | 20.8 |
| Phenacetin | 10.0 | 16.9 | 9.9 |
| Pimozide | 66.0 | 2.6 | 105.6 |
| Pindolol | 6.0 | 9.8 | 10.2 |
| Pracinostat | 13.0 | 14.6 | 11.3 |
| Prazosin | 8.0 | 15.6 | 12.2 |
| Propafenone | 20.0 | 11.5 | 20.0 |
| Propranolol | 30.0 | 9.2 | 14.1 |
| Quinidine | 37.0 | 16.4 | 18.6 |
| Resminostat | 8.0 | 10.6 | 6.7 |
| Rifampicin | 6.0 | 72.2 | 15.8 |
| Risperidone | 13.0 | 6.0 | 23.5 |
| Semagacestat | 6.0 | 23.3 | 9.3 |
| Sildenafil | 110.0 | 15.8 | 34.8 |
| Spautin-1 | 40.0 | 36.1 | 35.1 |
| Sulfaphenazole | 29.0 | 16.5 | 15.3 |
| Temozolomide | 13.0 | 20.1 | 4.8 |
| Testosterone | 210.0 | 21.0 | 100.4 |
| Ticlopidine | 45.0 | 171.4 | 55.4 |
| Tienilic Acid | 41.0 | 14.0 | 15.9 |
| Timolol | 6.0 | 6.5 | 8.3 |
| Tolbutamide | 6.0 | 10.3 | 8.0 |
| Tranlycypromine | 6.0 | 24.1 | 16.8 |
| Troglitazone | 82.0 | 6.2 | 95.3 |
| Warfarin | 6.0 | 8.3 | 9.2 |
| Venetoclax | 23.0 | 2.4 | 45.8 |
| Verapamil | 200.0 | 79.8 | 94.9 |

CL_{int} = in vitro intrinsic clearance; HLM = human liver microsomes

Supplemental Table 3.

Measured Caco-2 P_{app} and predicted P_{app} from the in-house model for a set of reference compounds. Data is the mean of at least three independent experiments.

| Compound | Measured Caco-2 P_{app} (10^{-6} cm/s) | Predicted Caco-2 P_{app} (In-house model, 10^{-6} cm/s) |
|-----------------------------|--|---|
| Abexinostat | 0.7 | 2.8 |
| Aliskiren | 0.2 | 1.2 |
| Atazanavir | 5.3 | 8.0 |
| Atenolol | <1 | 1.0 |
| Belinostat | 5.9 | 11.8 |
| Cyclopropavir | 1.0 | 1.1 |
| Degrasyn | 4.9 | 19.7 |
| Digoxin | 1.0 | 1.1 |
| Flupentixol | 5.7 | 11.9 |
| Ibudilast | 43.0 | 23.7 |
| Mepazine | 16.0 | 14.8 |
| Midazolam | 42.0 | 18.6 |
| Panobinostat | 0.8 | 1.8 |
| Phenacetin | 47.0 | 20.6 |
| Pimozide | 12.0 | 12.4 |
| Pracinostat | 2.5 | 3.8 |
| Propranolol | 17.9 | 10.4 |
| Resminostat | 5.2 | 2.3 |
| Rifampicin | 12.0 | 3.7 |
| Semagacestat | 4.0 | 1.3 |
| Sotrastaurin | 3.3 | 4.1 |
| Spautin-1 | 24.0 | 16.7 |
| Thioridazine | 18.0 | 13.5 |
| Tracedinaline | 8.4 | 13.2 |
| Venetoclax | 1.0 | 1.8 |
| Z-Vrpr-Fmk (Malt Inhibitor) | 1.0 | 0.9 |

P_{app} = apparent permeability

Supplemental Table 4.

Analysis of variance for log transformed data shown in Supplemental Tables 2 and 3.

| Assay | | Coefficients | Standard error | t-ratio | P-value | Lower 95% | Upper 95% |
|--|-----------|---------------------|-----------------------|----------------|----------------|------------------|------------------|
| Caco-2 (in house model versus measured values) | Intercept | 0.260 | 0.076 | 3.42 | 0.002 | 0.103 | 0.418 |
| | Slope | 0.667 | 0.083 | 8.01 | 3.11E-08 | 0.495 | 0.839 |
| HLM (global model versus measured values) | Intercept | 0.825 | 0.108 | 7.63 | 7.03E-11 | 0.610 | 1.04 |
| | Slope | 0.280 | 0.081 | 3.45 | 0.001 | 0.118 | 0.442 |
| HLM (in house model versus measured values) | Intercept | 0.568 | 0.084 | 6.74 | 3.21E-09 | 0.400 | 0.737 |
| | Slope | 0.555 | 0.063 | 8.75 | 5.37E-13 | 0.428 | 0.681 |